ELSEVIER

Nuclear Physics A704 (2002) 223c–231c

NUCLEAR PHYSICS A

www.elsevier.com/locate/npe

Shell model description of correlations in ^{56}Ni and ^{100}Sn

F. Nowacki[a]

[a]Laboratoire de Physique Théorique, 3-5 rue de l'Université,
67084 Strasbourg-Cedex, France.

Through a set of large scale shell model calculations, we illustrate the influence of correlations on several basic observables. In the ^{56}Ni region (fp shell), and the ^{100}Sn region (gds shell) we start from a single particle picture, the valence space is enlarged and eigenstates energies, electromagnetic rates are studied as a function of particle-hole excitations. Very similar behaviour is expected for the nature of ^{100}Sn and ^{56}Ni.

1. Introduction

Recent improvements have been achieved in the standard shell model technology and together with the use of more powerful computers, it is now possible to handle matrices of the order of 10^8 (m-scheme dimension, see E. Caurier 's contribution to this symposium). Nevertheless, this is not always sufficient in particular for the study of heavier systems, in the A$\sim$ 100 region for example. Through a set of calculations, we will make a parallel study of two distinct regions: the first one is ^{56}Ni and the surrounding nuclei, where full space calculations are feasible or almost. The second one is ^{100}Sn and its surrounding nuclei, where more drastic truncations of the valence space have to be employed. We will aim at comparing the effect of core excitations in both cases and derive some predictions for the behaviour of ^{100}Sn.

In order to study core excitations near the doubly magic ^{56}Ni and ^{100}Sn nuclei, we need to define two model spaces. For ^{56}Ni, we choose ^{40}Ca as closed core and include all neutron and protons orbits defined by the fp-shell. For ^{100}Sn, we choose as closed-shell core for the calculation ^{80}Zr and will consider valence neutrons and protons in the single-particle orbits $2s_{1/2}$, $1d_{5/2}$, $1d_{3/2}$, $0g_{7/2}$ and $0g_{9/2}$ (gds-shell). The effective interaction, provided by the Oslo group [1], is derived with standard many-body techniques (details are given in [2]). The monopole part has been modified to reproduce the observed experimental gaps and shell closures. For the fp-shell, this region has been investigated for many years now, and the monopole behaviour is therefore well determined, see for example Ref. [3]. The effective interaction we use, with the adequate monopole corrections, reproduces the shell gaps in ^{48}Ca and ^{56}Ni and the spectra of ^{49}Ca and ^{57}Ni. In the ^{100}Sn region, the experimental information is not so abundant. But some extrapolations from heavier Sn isotopes to ^{100}Sn (^{100}Sn shell gap and ^{101}Sn spectrum) can be made. The interaction we use was modified to reproduce shell gaps for ^{90}Zr, ^{100}Sn and the extrapolated spectrum of ^{101}Sn, see Ref. [4]. Since there is no experimental information on the single-particle spectrum of ^{80}Zr, which is our closed-shell core for the $A = 100$ calculation, we adopt the

PII S0375-9474(02)00782-0

Table 1
2_1^+ excitation energy and E2 transition rates to the ground state for selected Ni isotopes.

ph	0	1	2	3	4	5	6	Expt
^{56}Ni								
E(2^+)(MeV)	-	4.74	6.67	4.44	4.39	3.87	3.68	2.70
B(E2)(e^2.fm^4)	-	78	88	107	121	130	136	120±24
^{58}Ni								
E(2^+)(MeV)	1.12	1.14	1.33	1.29	1.34	1.36		1.45
B(E2)(e^2.fm^4)	10	40	43	63	73	85		135±3
^{60}Ni								
E(2^+)(MeV)	0.89	0.91	1.06	1.03	1.06			1.33
B(E2)(e^2.fm^4)	19	62	77	104	120			188±3

predicted ones from the global fit of all available single-particle and single-hole energies of Duflo and Zuker [5]. These are $\epsilon_{g_{\frac{9}{2}}}$=0.0 MeV, $\epsilon_{g_{\frac{7}{2}}}$=4.95 MeV, $\epsilon_{d_{\frac{5}{2}}}$=2.54 MeV, $\epsilon_{d_{\frac{3}{2}}}$=4.53 MeV, and $\epsilon_{s_{\frac{1}{2}}}$=3.34 MeV.

2. Results for the ^{56}Ni region

In Table 1, we show the evolution of the 2_1^+ excitation energy and E2 rate to the ground state, for ^{56}Ni, ^{58}Ni and ^{60}Ni as function of the number of particle-hole excitations. We focus first on ^{56}Ni. The 2_1^+ 1ph component is evidently of pure quadrupole nature and is therefore strongly connected through the E2 transition to the ground state (the standard polarization effective charge of 0.5e is used here for the calculation of electromagnetic transitions). Additional ph excitations will dress these two states through pairing-type correlations. When we add higher-order ph correlations, the 2^+ excitation decreases (with an odd-even staggering due to pairing) and the E2 transition strength to the ground state increases smoothly towards the experimental value. The actual discrepancy between the experimental and the calculated 2^+ excitation energy reflects the very slow convergence with the number of ph excitations. From Table 1, the 2^+ excitation energy is evidently not yet converged and one can expect additional corrections when adding 7p7h and higher correlations. Energy convergence of Yrast 0^+ and 2^+ states in ^{56}Ni can be estimated from Figure 1 where full space diagonalization where performed for the ground state and a 8p8h calculation was done for the first excited state. Full space diagonalization were also possible for excited 0^+ states and Figure 2 exhibits surprisingly fast energy convergence of the second and third states. This illustrates also the usefullness and descriptive power of truncated calculations with respect to other approximated methods [6,7]. The convergence of the E2 transition strength value is much faster and stabilizes at the 6 ph level. One can describe the 0_1^+ and 2_1^+ states in ^{56}Ni as 0ph and 1ph configurations which are perturbatively dressed with 2ph, 4ph pairing correlations. This is clear in Table

Table 2
Wave function components for the ground state and the first excited state in selected Ni isotopes.

ph(per cent.)	0	1	2	3	4
^{56}Ni					
0^+	66	-	26	3	5
2^+	-	45	14	24	9
^{58}Ni					
0^+	55	13	22	6	3
2^+	52	16	20	7	3
^{60}Ni					
0^+	54	20	19	5	2
2^+	51	23	18	6	2

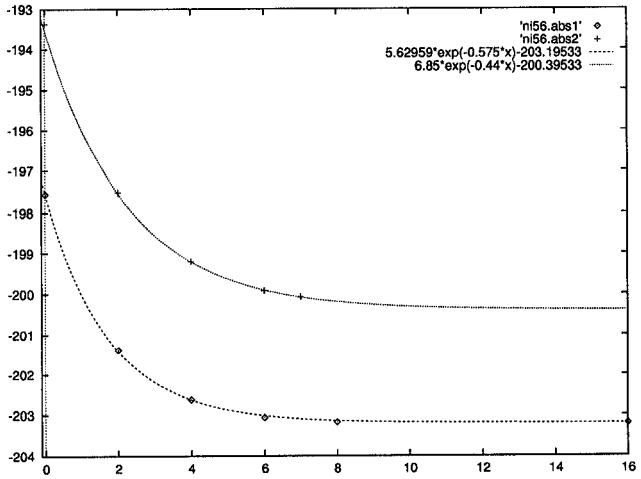

Figure 1. Energy convergence (in MeV) of the first two states in ^{56}Ni with the number of ph excitations (FPD6 interaction).

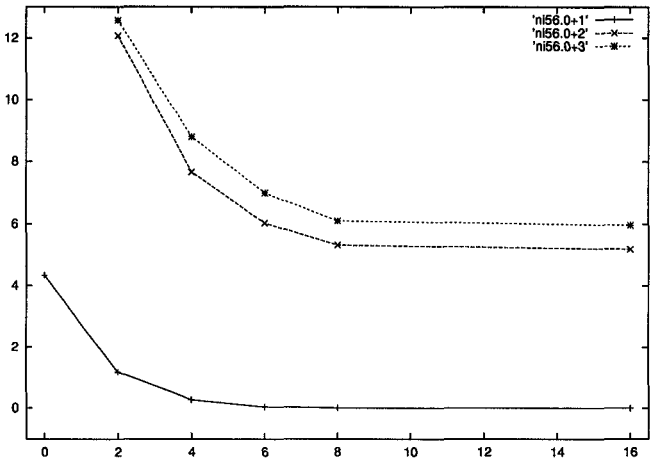

Figure 2. Excitation energy convergence (in MeV) of the first three 0^+ states in ^{56}Ni with the number of ph excitations.

2 where the leading 'dressing' configurations are of the 2 ph and 3 ph type for the 0_1^+ and 2_1^+ states, respectively (these correlations are extracted from the largest spaces achieved in Table 1).

To explicit in another way this dressing mechanism, we generate a deformed collective state by computing a pure 4 ph state. This state is not physical and we generate then (with the Whitehead method) a structure function in the 0+2+4+6 ph space. Figure 3 shows that the second and third states collect the largest amount of the strength, confirming the collective deformed nature of these two states. Notice that the ground state collects almost no strength (less than 0.5 per cent). Then we compute the 30 first 0^+ states (in the same space where the structure function was obtained) and extract the amount of 4p4h component. Again, the second and third states collects the largest amount, coinciding with the deformed previous components. But the ground state exhibit also some 4 ph correlations but not of deformed nature (but more likely of pairing nature).

For the other two nuclei ^{58}Ni and ^{60}Ni, the mechanism is essentially a coupling to the 2_1^+ 1 ph components of ^{56}Ni. Then these basic configurations are dressed again through pairing-type correlations. But the effect is the opposite, the zero-order 0ph configuration gives a very small quadrupole transition and the coupling of these two configurations to the 1 ph excitations of ^{56}Ni enhances strongly the E2 transition. Then higher-order ph correlations increase smoothly but the 2^+ excitation energy no longer staggers as both 0^+ and 2^+ have the same zero order configuration. Table 2 shows again the dressing mechanism for ^{58}Ni and ^{60}Ni.

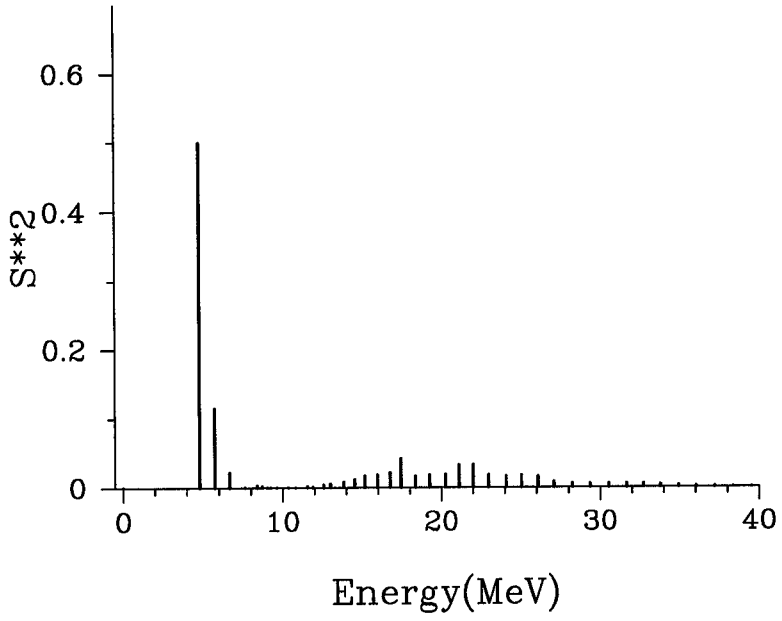

Figure 3. Structure function of the deformed collective pure 4 ph 0^+ state in the 0+2+4+6 ph space.

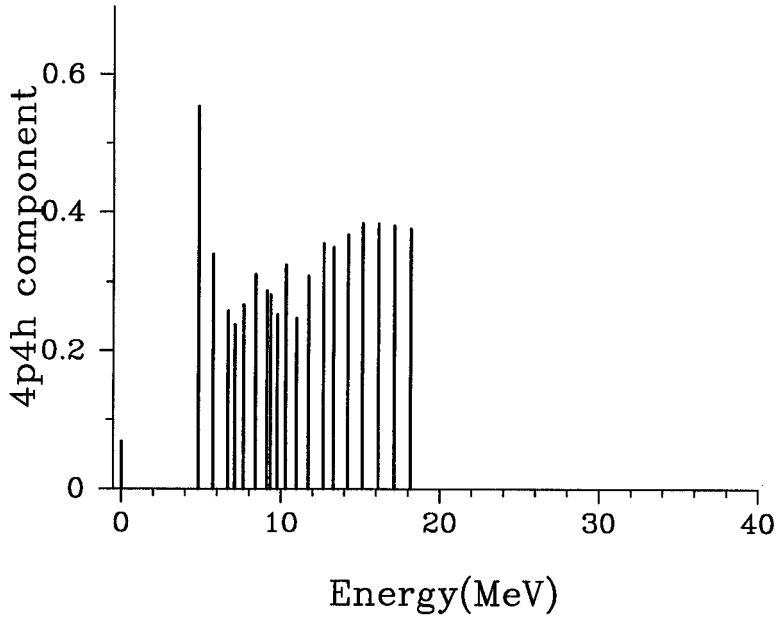

Figure 4. 4 ph components in the 30 first 0^+ states of ^{56}Ni.

3. Results for the ^{100}Sn region

We are now moving to the ^{100}Sn region and will produce the same kind of calculations. The size of the valence space prohibits full $0\hbar\omega$ calculations but with restricted calculations and experience from *fp* shell, we will describe the behaviour expected for ^{100}Sn.

Table 3 shows the 2_1^+ excitation energy and $2_1^+ \rightarrow 0_1^+$ transition for ^{100}Sn, ^{102}Sn and ^{104}Sn. Due to the large shell-model dimensionality, we are forced here to retain a more moderate number of ph excitations: the valence space is extended up to 4 ph excitations in ^{100}Sn, 3 ph excitations in ^{102}Sn and up to 3 ph (with only one particle in the $1d_{3/2}$, $2s_{1/2}$ orbitals) excitations in ^{104}Sn. However, these excitations are sufficient in order to illustrate the mechanism seen in the Ni isotopes. The single particle picture is identical to the one in ^{56}Ni, i.e., the ground state consists of doubly closed shells and the 2^+ state has a pure particle-hole quadrupole component. Then, the introduced correlations essentially interact through pairing components. Table 3 shows that the behaviour is similar to that seen in Table 2. In particular, for the case of ^{100}Sn, the staggering of the 2_1^+ excitation energy behaves very closely to the one in ^{56}Ni, suggesting identical nature of these two nuclei. The 2_1^+ in ^{100}Sn is therefore expected to lie at the value close to the one in ^{56}Ni (roughly 3 MeV).

The recent data accumulated in the region do not contain yet the low-lying states exposed previously but concern the structure of high-spin states in ^{98}Cd, ^{102}Sn, ^{104}Sn [10,8,9]. In particular, a large E2 strength in the Sn isotopes [8,9] and the retarded B(E2) in ^{98}Cd [10] have been observed experimentally. In Table 4, we produce the comparison of the accumulated data and our calculations. The results are convincing and do show the influence of core excitations on the observed accelerated E2 transitions. They also give confidence in the extrapolations drawn for low-lying states. In the case of ^{98}Cd (not shown here), a spin-trap isomer explains the retarded B(E2) observed there.

Table 3
2_1^+ excitation energy and E2 transition rates to the ground state for Sn isotopes. The label * refer to one particle in $d_{\frac{3}{2}}s_{\frac{1}{2}}$ only.

ph	0	1	2	3	4	Expt
^{100}Sn						
$E(2^+)$(MeV)	-	4.8	6.30	4.58	4.56	
$B(E2)(e^2.fm^4)$	-	196	219	251	270	
^{102}Sn						
$E(2^+)$(MeV)	1.05	1.1	1.24	1.22		1.47
$B(E2)(e^2.fm^4)$	19	79	93	137		
^{104}Sn						
$E(2^+)$(MeV)	0.86	0.82	0.84	0.79*		1.26
$B(E2)(e^2.fm^4)$	41	143	192	209*		

Table 4
High-spin gamma transitions and E2 rates in ^{102}Sn and ^{104}Sn. The label * stands for one particle in $d_{\frac{3}{2}}s_{\frac{1}{2}}$ only.

ph	0	1	2	3	Expt
^{102}Sn					
E(6^+)-E(4^+)(MeV)	0.102	0.031	0.039	0.023	0.048
B(E2)($e^2.fm^4$)	7.2	40	49	73	$116\pm^{70}_{30}$
E(10^+)-E(8^+)(MeV)	-	0.74	0.67	0.68	
B(E2)($e^2.fm^4$)	-	65	137	198	
^{104}Sn					
E(6^+)-E(4^+)(MeV)	0.28	0.47	0.58	0.56*	0.31
B(E2)($e^2.fm^4$)	4	50	77	87*	119 ±16
E(10^+)-E(8^+)(MeV)	0.63	0.64	0.68	0.61*	0.54
B(E2)($e^2.fm^4$)	7	51	79	82*	119 ±17

4. Summary and conclusion

We have studied the effect of core polarization on energies and the E2 strength in ^{56}Ni and ^{100}S. The structure looks very similar in both regions. Using a canonical polarization effective charge of 0.5e, the observed E2 transitions can be interpreted as np-nh excitations on a double-shell closed core.

5. Acknowledgments

The results presented in this contribution have been obtained in collaboration with E. Caurier, H. Grawe, M. Hjorth-Jensen and G. Martinez-Pinedo.

REFERENCES

1. M. Hjorth-Jensen, private communication.
2. M. Hjorth-Jensen, T. T. S. Kuo and Eivind Osnes, Phys. Rep. **261** (1995) 125.
3. E. Caurier, A. P. Zuker, A. Poves, and G. Martínez-Pinedo, Phys. Rev. C**50** (1994) 225.
4. H. Grawe *et al.*, in 'Highlights of Modern Nuclear Structure', edited by A. Covello, (World Scientific, Singapore, 1999) p. 137.
5. J. Duflo and A. P. Zuker, Phys. Rev. **C59** (1999) 2347.
6. S. E. Koonin, D. J. Dean and K. Langanke, Phys. Rep. **278** (1997) 1.
7. T. Otsuka, M. Honma, and T. Mizusaki, Phys. Rev. Lett. **81** (1998) 1588.
8. M. Gorska *et al.*, Phys. Rev. C **58**, 108 (1998).
9. M. Lipoglavsek *et al.*, Phys. Lett. **440B**, 246 (1998).
10. M. Gorska *et al.*, Phys. Rev. Lett. **79**, 2415 (1997).